Structure Dependence of Excitonic Effects in Chiral Graphene Nanoribbons *

Yan Lu(吕燕)[1], Wen-Gang Lu(吕文刚)[2,3]**, Li Wang(王立)[1]**

[1]*Department of Physics, Nanchang University, Nanchang 330031*

[2]*Beijing National Laboratory for Condensed Matter Physics, and Institute of Physics, Chinese Academy of Sciences, Beijing 100190*

[3]*Beijing Key Laboratory for Nanomaterials and Nanodevices, Beijing 100190*

(Received 18 October 2016)

We explore the excitonic effects in chiral graphene nanoribbons (cGNRs), whose edges are composed alternatively of armchair-edged and zigzag-edged segments. For cGNRs dominated by armchair edges, their energy gaps and exciton energies decrease with increasing chirality angles, and they, as functions of widths, oscillate with the period of three, while the exciton binding energies do not have such distinct oscillation. On the other hand, for cGNRs dominated by zigzag edges, all the energy gaps, exciton energies, and exciton binding energies show oscillation properties with their widths, due to the interactions between the edge states localized at the opposite zigzag edges. In addition, the triplet excitons are energy degenerate when the electrons are spin-unpolarized, while the degeneracy split when the electrons are spin-polarized. All the studied cGNRs show strong excitonic effects with the exciton binding energies of hundreds of meV.

PACS: 71.35.−y, 73.22.−f, 62.23.Hj DOI: 10.1088/0256-307X/34/1/017102

The zero-energy-gap property of graphene hinders its use in photoelectric applications.[1,2] One way to open an energy gap in graphene is to lower its dimension to one-dimensional (1D) nanoribbons.[3–7] Among them, armchair-edged graphene nanoribbons (aGNRs) and zigzag-edged graphene nanoribbons (zGNRs) are two typical kinds of graphene nanoribbons (GNRs). In addition to these two typical kinds of GNRs, the GNRs with the edges along ribbon directions alternatively being armchair edges and zigzag edges are called chiral GNRs (cGNRs). Theoretically, Jaskolski *et al.*[8] showed the existence of edge states and flat bands in cGNRs. Further calculations showed that these edge states will be spin-polarized in the presence of the Hubbard interactions[9–13] and affect optical absorptions in cGNRs.[14] However, these calculations have not included the excitonic effects. Actually, excitons, bound states of electron–hole (e–h) pairs, have shown the importance in optical properties of low-dimensional materials,[15–20] because the low dimensional structures enhance electron–electron (e–e) and e–h interactions. In this work, using the spin-polarized tight-binding (TB) method and including e–e interactions, we investigate the electronic properties and excitonic effects of cGNRs with various sizes.

We apply the TB Pariser–Parr–Pople (PPP) model[21] to investigate the excitonic effects in cGNRs.[16,18,22–24] The PPP Hamiltonian is given by[18]

$$H = H_0 + H_{\mathrm{e-e}}, \tag{1}$$

$$H_0 = t\sum_{\langle i,j\rangle,\sigma} c^{\dagger}_{i\sigma}c_{j\sigma} + \sum_{i,\sigma} U\Big(\langle n_{i\bar{\sigma}}\rangle - \frac{1}{2}\Big)n_{i\sigma}, \tag{2}$$

$$\begin{aligned} H_{\mathrm{e-e}} = {} & U\sum_i (n_{i\uparrow} - \langle n_{i\uparrow}\rangle)(n_{i\downarrow} - \langle n_{i\downarrow}\rangle) \\ & + \frac{1}{2}\sum_{i,j(i\neq j)}\sum_{\sigma,\sigma'} V_{ij}(n_{i\sigma} \\ & - \langle n_{i\sigma}\rangle)(n_{j\sigma'} - \langle n_{j\sigma'}\rangle), \end{aligned} \tag{3}$$

where H_0 is the spin-resolved TB Hamiltonian, $H_{\mathrm{e-e}}$ denotes the e–e interactions, $\langle i,j\rangle$ means that i and j are nearest neighbor sites, $c^{\dagger}_{i\sigma}$, $c_{i\sigma}$, and $n_{i\sigma}$ are the electron creation, annihilation, and number operators on site i with spin σ, respectively, $\langle n_{i\sigma}\rangle$ is the average occupation probability of spin σ electrons on site i, and t and U are the nearest-neighbor hopping and on-site Hubbard interaction, respectively. Here V_{ij} is the long-range Coulomb interactions, which takes Ohno's formula[25]

$$V_{ij} = \frac{U}{\kappa\sqrt{1 + (\frac{4\pi\epsilon_0}{e^2}Ur_{ij})^2}}, \tag{4}$$

where ϵ_0 and e are the vacuum permittivity and the magnitude of the electron charge, respectively, r_{ij} is the distance between sites i and j in units of Å, and κ is the dielectric function and introduced to incorporate the screening effects from the environment and the σ electrons in cGNRs. In our calculations, the three independent parameters are chosen as $t = -2.6$ eV, $U = 2.75$ eV and $\kappa = 2.1$, which are exactly the same as chosen in our previous calculations of excitonic effects in zGNRs.[18] Other parameters have also been tested and shown only quantitative but not qualitative change of our results.

*Supported by the National Key Scientific Research Projects of China under Grant No 2015CB932400, the National Natural Science Foundation of China under Grant Nos 11504158, 61474059, and U1432129, the Program for New Century Excellent Talents in University of Ministry of Education of China under Grant No NCET-11-1003, and the Jiangxi Provincial 'Ganpo Talentes 555 Projects'.

**Corresponding author. Email: wglu@iphy.ac.cn; liwang@ncu.edu.cn

© 2017 Chinese Physical Society and IOP Publishing Ltd

Exciton states, denoted as $|\mathrm{ex}\rangle$, are expressed as a linear combination of single e–h pair excitation states, i.e., $|\mathrm{ex}\rangle = \sum_{\boldsymbol{k}_\mathrm{c},\boldsymbol{k}_\mathrm{v}} \rho(\boldsymbol{k}_\mathrm{c},\boldsymbol{k}_\mathrm{v})|\boldsymbol{k}_\mathrm{c},\boldsymbol{k}_\mathrm{v}\rangle$, where $\rho(\boldsymbol{k}_\mathrm{c},\boldsymbol{k}_\mathrm{v})$ is the weight coefficient, $\boldsymbol{k}_\mathrm{c}$ ($\boldsymbol{k}_\mathrm{v}$) denotes the wave vector of electrons in conduction (valence) bands, and $|\boldsymbol{k}_\mathrm{c},\boldsymbol{k}_\mathrm{v}\rangle$ is the single e–h pair state. If spins are taken into account, there are four exciton states: one for singlet (S) and three for triplets (T_0, T_1, and T_{-1}). Specifically, we have[23,26]

$$|\boldsymbol{k}_\mathrm{c},\boldsymbol{k}_\mathrm{v}\rangle = \begin{cases} \frac{1}{\sqrt{2}}(|\boldsymbol{k}_\mathrm{c}\uparrow,\boldsymbol{k}_\mathrm{v}\uparrow\rangle + |\boldsymbol{k}_\mathrm{c}\downarrow,\boldsymbol{k}_\mathrm{v}\downarrow\rangle), & S, \\ \frac{1}{\sqrt{2}}(|\boldsymbol{k}_\mathrm{c}\uparrow,\boldsymbol{k}_\mathrm{v}\uparrow\rangle - |\boldsymbol{k}_\mathrm{c}\downarrow,\boldsymbol{k}_\mathrm{v}\downarrow\rangle), & T_0, \\ |\boldsymbol{k}_\mathrm{c}\uparrow,\boldsymbol{k}_\mathrm{v}\downarrow\rangle, & T_1, \\ |\boldsymbol{k}_\mathrm{c}\downarrow,\boldsymbol{k}_\mathrm{v}\uparrow\rangle, & T_{-1}. \end{cases} \quad (5)$$

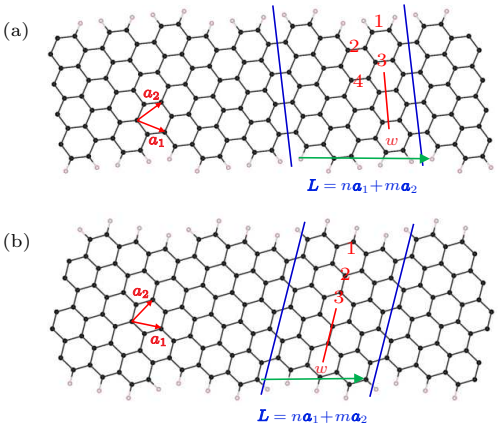

Fig. 1. Structures of (a) (3,2) cGNR and (b) (3,1) cGNR.

In Fig. 1 we plot the structures of two specific cGNRs whose unit cells are slightly tilted from a ZGNR and an aGNR, respectively. A vector $\boldsymbol{L} = n\boldsymbol{a}_1 + m\boldsymbol{a}_2$ is introduced to describe the edge-orientation of cGNRs, where $\boldsymbol{a}_1$ and $\boldsymbol{a}_2$ are the two lattice vectors of graphene. Since one integer pair (n,m) specifies one cGNR, $\boldsymbol{L}$ is defined as a chiral vector. The angle between vectors $\boldsymbol{L}$ and $\boldsymbol{a}_1$ is defined as the chirality angle θ, and expressed as

$$\theta = \arccos\left(\frac{2n+m}{2\sqrt{n^2+nm+m^2}}\right). \quad (6)$$

Obviously, the zGNRs and aGNRs have chirality angles of $\theta = 0°$ and $\theta = 30°$, respectively, and $0° < \theta < 30°$ for other cGNRs. The basic repeating unit, marked with the two blue dashed lines in Fig. 1, can be described by a unit vector $\boldsymbol{L}$. The length of $\boldsymbol{L}$ is $L = \sqrt{n^2+nm+m^2}a_0$, where $a_0 = 0.246\,\mathrm{nm}$ is the lattice constant of graphene.

In addition to the two integers of (n,m), it is necessary to introduce another integer w to denote the width of cGNRs. The value of w in $(n,1)$ cGNRs is defined by the number of zigzag carbon atom chains within a unit cell. In $(n,n-1)$ cGNRs, the value of w is defined by the number of carbon–carbon dimer lines as shown in Fig. 1(b).

At the beginning, we briefly discuss the TB energy bands of the two kinds of cGNRs calculated by H_0 in Eq. (2). For the $(n,n-1)$ cGNRs, the example bands of (4,3), (3,2) and (2,1) cGNRs are plotted in Fig. 2. The lowest conduction subband (CB1) and the highest valence subband (VB1), are edge states, mainly localized on the zigzag edges. Because the armchair-edged segments are dominant, and the zigzag-edged only occupy a very small portion, these edge states will not go through spin-polarization for the value of U ($U = 2.75\,\mathrm{eV}$) in our calculations. However, when U is large enough, these edge states can be spin-polarized.[9]

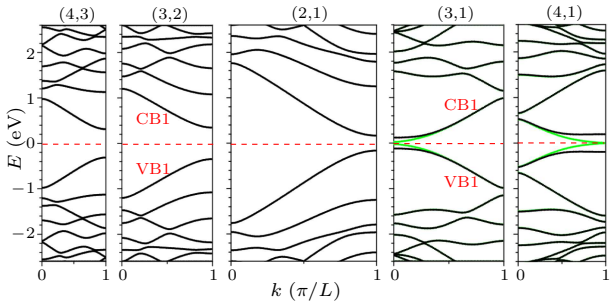

Fig. 2. TB band structures for (4,3), (3,2), (2,1), (3,1), and (4,1) cGNRs. The values of the width numbers are $w = 9$ for the (4,3), (3,2), and (2,1) cGNRs, and $w = 6$ for the (3,1) and (4,1) cGNRs. The red dashed lines denote the positions of the Fermi energies. The green bands are calculated without the Hubbard interaction ($U = 0$), and the black bands are calculated with the Hubbard interaction ($U = 2.75\,\mathrm{eV}$).

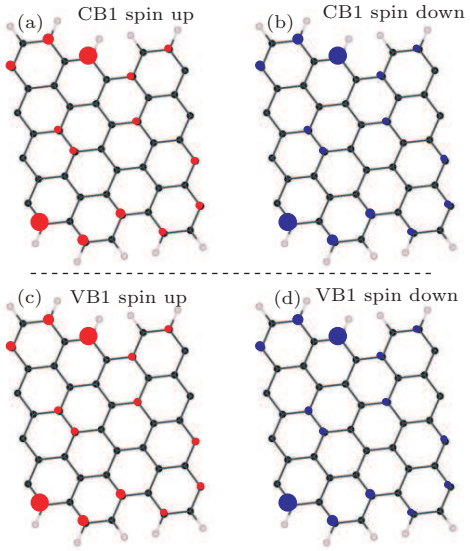

Fig. 3. The distributions of the electrons in (a) CB1 for up-spin, (b) CB1 for down-spin, (c) VB1 for up-spin, and (d) VB1 for down-spin of the (3,2) cGNR with $w = 9$.

For $(n,1)$ cGNRs, the bands of examples (3,1) and (4,1) cGNRs show that the CB1 and VB1 are mainly edge states localized at the zigzag edges, like the above $(n,n-1)$ case. When the Hubbard interaction is not taken into account ($U = 0$), the edge states in the CB1 and VB1 will touch with each other at the Fermi energy, as shown by the green lines in Fig. 2. This results in relatively large density of states at the Fermi energy. When the Hubbard interaction is taken into

account ($U = 2.75$ eV), the two touched edge states will be split and energy gaps are opened. Therefore, with present U, $(n, n-1)$ cGNRs are spin-unpolarized while $(n, 1)$ cGNRs are spin-polarized.

The charge distributions of the spin-unpolarized and spin-polarized edge states are different. We plot the electron distributions of CB1 and VB1 of two kinds of cGNRs, (3,2) and (3,1), in Figs. 3 and 4, respectively. In Fig. 3, the distributions are spin-independent, in accordance with the spin-unpolarized property in these two subbands, and the distributions of electrons in VB1 and in CB1 are the same, due to the electron–hole symmetry under the nearest-neighbour TB approximation.

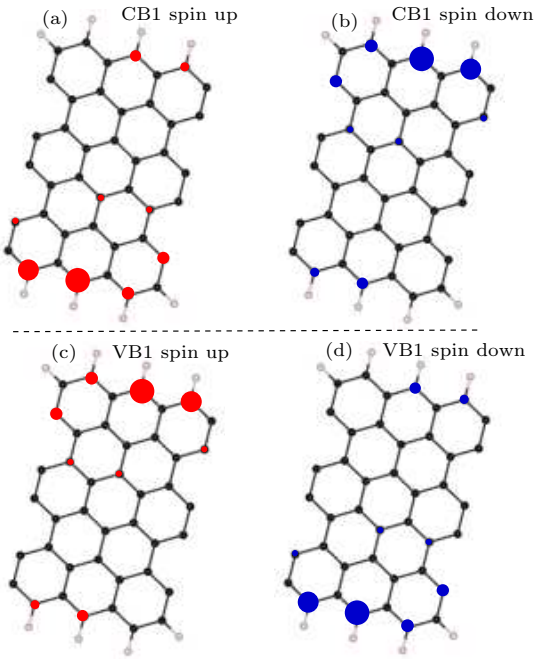

Fig. 4. The distributions of the electrons in (a) CB1 for up-spin, (b) CB1 for down-spin, (c) VB1 for up-spin, and (d) VB1 for down-spin of the (3,1) cGNR with $w = 6$.

The distributions of the (3,1) cGNR, plotted in Fig. 4, are totally different from those of the (3,2) cGNR. Figure 4(a) plots the distributions of spin-up electrons in CB1, which are mostly localized at one zigzag edge. On the other hand, the distributions of spin-down electrons in CB1 are localized at the other zigzag edge. These spin-dependent distributions mean that the electrons in the CB1 subband are spin-polarized. Similarly, the distributions of electrons in VB1 are also spin-dependent, as shown in Figs. 4(c) and 4(d). Importantly, the spin distributions of electrons in the VB1 are different from those in the CB1. As shown in the figure, electrons with up-spin in VB1 are localized at the same edge as those with down-spin in CB1. In other words, the electrons with one spin in VB1 and with the other spin in CB1 are localized at the opposite edges. These distribution differences of the spin-unpolarized and spin-polarized cGNRs may result in different excitonic effects.

By calculating the excitonic eigenvalue equations, we can obtain the renormalized energy gaps, exciton energies, and exciton binding energies in cGNRs. The calculated results for some cGNRs are shown in Fig. 5. For the $(n, n-1)$ cGNRs with the width $w = 9$, the TB energy gap $E_{\rm g}^{H_0}$, calculated by H_0 and shown by the green square-dotted line in Fig. 5(a) decrease with increasing n, which agree with previous calculations.[27] Based on the definition of the chiral angle θ, the TB energy gap decreases as θ increases. When the e–e Hamiltonian in Eq. (3) is taken into account, the renormalized energy gap $E_{\rm g}^{H}$, calculated by H and plotted with the pink diamond-dotted line, has the same trend as $E_{\rm g}^{H_0}$, while the magnitudes are about 0.7 eV higher. This property shows that many-body effects are quite strong in cGNRs. Furthermore, when the excitonic effects are taken into account, some low exciton energy levels appear within the renormalized energy gaps. As shown in Fig. 5(a), the line of the lowest energy levels of singlet excitons ($E_{\rm S}$) has the same trend as $E_{\rm g}^{H}$ and is about 0.4 eV lower. Therefore, the corresponding exciton binding energies ($E_{\rm b}^{\rm S}$) for these excitons are about 0.4 eV, showing strong exciton effects in cGNRs. However, as shown by the figure, $E_{\rm b}^{\rm S}$ decreases slowly compared with $E_{\rm g}^{H_0}$, $E_{\rm g}^{H}$ and $E_{\rm S}$, due to the fact that the widths of the cGNRs are fixed with increasing n.

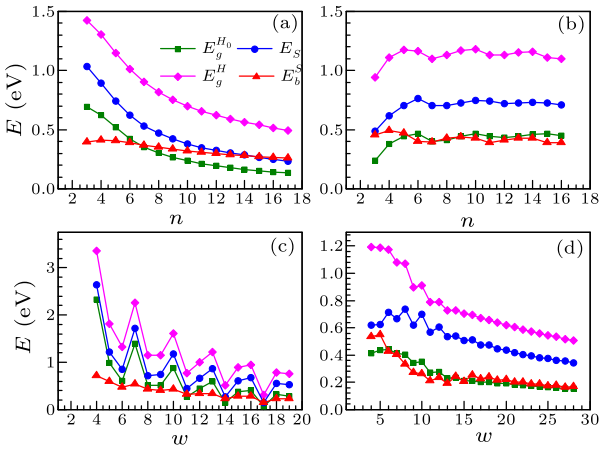

Fig. 5. TB energy gaps ($E_{\rm g}^{H_0}$), renormalized energy gaps ($E_{\rm g}^{H}$), lowest exciton energy of singlet ($E_{\rm S}$) and the corresponding exciton binding energies ($E_{\rm b}^{\rm S}$) as a function of (a) the value of n in the $(n, n-1)$ cGNRs with $w = 9$, (b) the value of n in the $(n, 1)$ cGNRs with $w = 6$, (c) the width number w for the $(5, 4)$ cGNR, and (d) the width number w for the $(5, 1)$ cGNR.

The energies for $(n, 1)$ cGNRs are quite different from those of $(n, n-1)$ cGNRs. As shown in Fig. 5(b), when n increases, $E_{\rm g}^{H_0}$ does not decrease or increase monotonously, but increases first and then oscillates around 0.45 eV, which equals to the energy gaps of zGNRs with the same widths. This is because the edge-localized magnetic moments will quickly converge to those of zGNRs when the lengths of zigzag edges of $(n, 1)$ cGNR increase. Here $E_{\rm g}^{H}$ and $E_{\rm S}$ have similar trends to $E_{\rm g}^{H_0}$, while they are about 0.7 eV and 0.3 eV larger than $E_{\rm g}^{H_0}$, respectively, and $E_{\rm b}^{\rm S}$ is much flatter

with almost unchanged values.

Next, the width-dependent exciton effects are investigated. When the width of an $(n, n-1)$ cGNR increases, $E_{\rm g}^{H_0}$, $E_{\rm g}^{H}$ and $E_{\rm S}$ oscillate distinctively with the period of three, such as the (5,4) cGNR shown in Fig. 5(c). Generally, the energy gaps are the largest when $\mathrm{mod}(w,3)=1$, the smallest when $\mathrm{mod}(w,3)=2$, and medium when $\mathrm{mod}(w,3)=0$. This property is similar to the oscillation of the energy gaps of aGNRs because of their structure similarity.[28] The oscillation property can be understood by three kinds of projections of the 2D band structure of graphene onto the 1D Brillouin zone of the $(n, n-1)$ cGNRs, as previous successful explanation of aGNRs. The values of $E_{\rm g}^{H_0}$, $E_{\rm g}^{H}$, and $E_{\rm S}$ plotted in Fig. 5(c) have the same oscillations, while $E_{\rm b}^{\rm S}$ shows a much small oscillation. This means that the binding energy is not very sensitive to the energy gap.

For the $(n,1)$ cGNRs, when the width increases, $E_{\rm g}^{H_0}$, $E_{\rm g}^{H}$, $E_{\rm S}$, and $E_{\rm b}^{\rm S}$ also show oscillations but with the period of two, as shown in Fig. 5(d). The period of two comes from the fact that there are two different symmetries between the opposite zigzag edges depending on whether w is odd or even, therefore there are two different couplings between the opposite edge states. The strengths of the couplings will damp out as the widths increase, due to the localized behavior of the edge states. As a result, these oscillations damp out. Then $E_{\rm g}^{H_0}$, $E_{\rm g}^{H}$, $E_{\rm S}$, and $E_{\rm b}^{\rm S}$ become smoother and decrease monotonously for large w, as shown in Fig. 5(d).

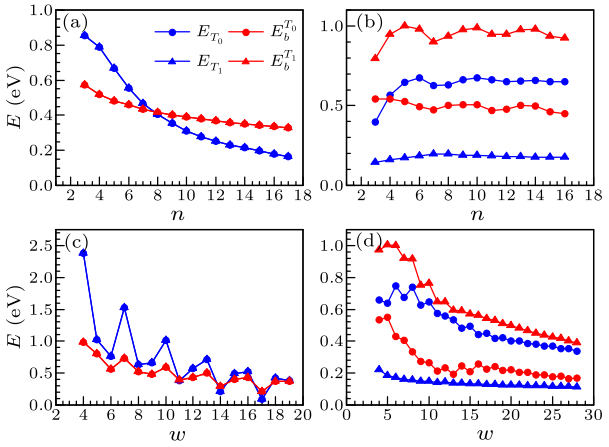

Fig. 6. The lowest energies for T_0 and T_1 triplets ($E_{\rm T0}$ and $E_{\rm T1}$), and the corresponding exciton binding energies ($E_{\rm b}^{\rm T0}$ and $E_{\rm b}^{\rm T1}$) as a function of (a) the value of n in the $(n, n-1)$ cGNRs with $w=9$, (b) the value of n in the $(n,1)$ cGNRs with $w=6$, (c) the width number w for the (5,4) cGNR, and (d) the width number w for the (5,1) cGNR.

Another difference between the exciton effects in spin-unpolarized and spin-polarized cGNRs is that the three triplet excitons are degenerate in energy for spin-unpolarized cGNRs but not for spin-polarized cGNRs, i.e., T_1 and T_{-1} triplets are degenerate for both kinds of cGNRs, while T_1 and T_{-1} triplets are not degenerate with T_0 triplet for spin-polarized cGNRs. Figure 6(a) plots the lowest energy levels for T_0 and T_1 triplets ($E_{\rm T0}$ and $E_{\rm T1}$) and the corresponding binding energies ($E_{\rm b}^{\rm T0}$ and $E_{\rm b}^{\rm T1}$) as a function of the value of n for the $(n, n-1)$ cGNRs. As is shown, the T_0 and T_1 triplets are energy degenerate since the electron distributions are spin-independent in these spin-unpolarized cGNRs. However, as shown in Fig. 6(b), T_0 and T_1 triplets are not degenerate to each other for the $(n,1)$ cGNRs. Here $E_{\rm T1}$ is smaller than $E_{\rm T0}$, and correspondingly, $E_{\rm b}^{\rm T1}$ is larger than $E_{\rm b}^{\rm T0}$. Figures 6(c) and 6(d) plot the width-dependent relationships of exciton energies and exciton binding energies showing the same degenerate relations of the triplets in $(n,1)$ cGNRs.

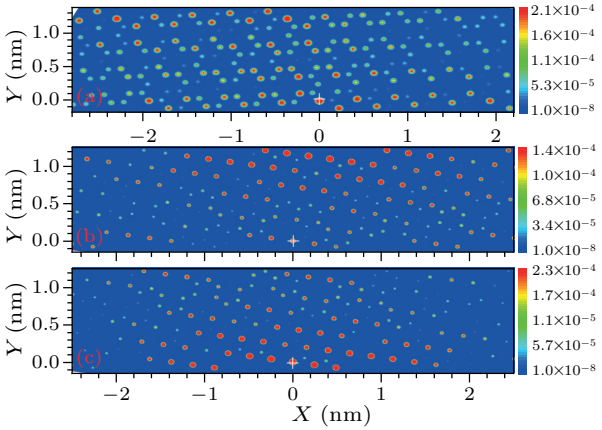

Fig. 7. Electron distributions of (a) the lowest state of S exciton for the (5,4) cGNRs with $w=12$, (b) the lowest state of T_0 exciton for the (5,1) cGNRs with $w=6$, and (c) the lowest state of T_1 exciton for the (5,1) cGNRs with $w=6$. The holes are fixed on the sites denoted by white crosses.

The reason for this energy splitting of triplets is the spin-dependent charge distributions in the $(n,1)$ cGNRs. It is known that the lowest energy excitons are mainly composed of the electrons in CB1 and holes in VB1. According to the discussion of Fig. 4, when an electron is excited from VB1 to CB1 without flipping its spin, the excited electron and the remaining hole will distribute at two opposite edges. However, if the spin is flipped during the excitation process, then the electron and hole are localized at the same edge. Therefore, there are two kinds of excitons depending on the spins of the electron and the hole. According to the definition of exciton states shown in Eq. (2), the spin is not flipped in T_0 exciton, but flipped in T_1 and T_{-1} excitons. Therefore, the electron and hole are at different edges for T_0 triplet, but at the same edges for T_1 and T_{-1} triplets. Obviously, the Coulomb attractions between the electron and the hole are larger in T_1 and T_{-1} triplets than in T_0 triplet, which results in much stronger exciton binding energies for T_1 and T_{-1} triplets, as plotted in Figs. 6(b) and 6(d).

In Fig. 7 we plot the electron distributions in three representative excitons. The holes are fixed on the sites having the largest probabilities. They all are on edge atoms and denoted by white crosses. The

electron in the lowest state of S exciton in the (5,4) cGNR will distribute with nearly equal probability at the two edges as shown in Fig. 7(a), since the edge states are spin-unpolarized in this cGNR. However, for the lowest state of T_0 exciton in the (5,1) cGNR, the electron prefers to distribute at the opposite edge of the hole, as shown in Fig. 7(b). For the lowest state of T_1 triplet, the electron prefers to distribute at the same edge around the hole. These electron distributions are consistent with our discussions in the above paragraph.

In conclusion, we have calculated the electronic properties and excitonic effects of cGNRs by using the spin-resolved TB method with e–e interactions. For the $(n, n-1)$ cGNRs which are dominated by armchair edges, their edge states are spin-unpolarized. The corresponding energy gaps, exciton energies, and exciton binding energies decrease when the portions of armchair edges in unit cells increase. As functions of the widths, the energy gaps and exciton energies oscillate with the period of three. For the $(n, 1)$ cGNRs which are dominated by zigzag edges, their energy gaps, exciton energies, and exciton binding energies also show oscillations with increasing widths, while this property is caused by the interactions between the edge states localized at the opposite zigzag edges. We also find that the triplet excitons are energy degenerate for cGNRs with spin-unpolarized edge states. However, this energy degeneracy is higher with spin-polarized edge states, which is caused by two kinds of exciton distributions of triplets in the presence of spin polarization.

References

[1] Novoselov K S, Geim A K, Morozov S V, Jiang D, Katsnelson M I, Grigorieva I V, Dubonos S V and Firsov A A 2005 *Nature* **438** 197

[2] Zhang Y, Tan Y W, Stormer H L and Kim P 2005 *Nature* **438** 201

[3] Han M Y, Özyilmaz B, Zhang Y and Kim P 2007 *Phys. Rev. Lett.* **98** 206805

[4] Son Y W, Cohen M L and Louie S G 2006 *Phys. Rev. Lett.* **97** 216803

[5] Wang X, Ouyang Y, Jiao L, Wang H, Xie L, Wu J, Guo J and Dai H 2011 *Nat. Nanotechnol.* **6** 563

[6] Li Y Y, Chen M X, Weinert M and Li L 2014 *Nat. Commun.* **5** 4311

[7] Wang W X, Zhou M, Li X, Li S Y, Wu X, Duan W and He L 2016 *Phys. Rev.* B **93** 241403(R)

[8] Jaskólski W, Ayuela A, Pelc M, Santos H and Chico L 2011 *Phys. Rev.* B **83** 235424

[9] Yazyev O V, Capaz R B and Louie S G 2011 *Phys. Rev.* B **84** 115406

[10] Sun L, Wei P, Wei J, Sanvito S and Hou S 2011 *J. Phys.: Condens. Matter* **23** 425301

[11] Golor M, Lang T C and Wessel S 2013 *Phys. Rev.* B **87** 155441

[12] Carvalho A R, Warnes J H and Lewenkopf C H 2014 *Phys. Rev.* B **89** 245444

[13] Jaskolski W and Ayuela A 2014 *Solid State Commun.* **196** 1

[14] Berahman M, Asad M, Sanaee M and Sheikhi M H 2015 *Opt. Quantum Electron.* **47** 3289

[15] Yang L, Cohen M L and Louie S G 2007 *Nano Lett.* **7** 3112

[16] Lu Y, Zhao S, Lu W, Liu H and Liang W 2014 *J. Appl. Phys.* **115** 103701

[17] Yang L, Cohen M L and Louie S G 2008 *Phys. Rev. Lett.* **101** 186401

[18] Lu Y, Lu W G, Liang W J and Liu H 2013 *Phys. Rev.* B **88** 165425

[19] Cheiwchanchamnangij T and Lambrecht W R L 2012 *Phys. Rev.* B **85** 205302

[20] Tran V, Soklaski R, Liang Y and Yang L 2014 *Phys. Rev.* B **89** 235319

[21] Pariser R and Parr R G 1953 *J. Chem. Phys.* **21** 466
Pople J A 1953 *Trans. Faraday Soc.* **49** 1375

[22] McWilliams P C M, Hayden G W and Soos Z G 1991 *Phys. Rev.* B **43** 9777 and references therein

[23] Abe S, Yu J and Su W P 1992 *Phys. Rev.* B **45** 8264

[24] Zhao H and Mazumdar S 2004 *Phys. Rev. Lett.* **93** 157402

[25] Ohno K 1964 *Theor. Chim. Acta* **2** 219

[26] Rohlfing M and Louie S G 2000 *Phys. Rev.* B **62** 4927

[27] Ezawa M 2006 *Phys. Rev.* B **73** 045432

[28] Jiang Z and Song Y 2015 *Physica* B **464** 61